

OPTIMIZED GAINS FOR THE CONTROL OF ISLANDED SOLAR PHOTOVOLTAIC AND WIND SYSTEM

Sravya KEDARI¹ , Rajagopal VERAMALLA¹ , Amritha KODAKKAL² 

¹Department of Electrical and Electronics Engineering, Kakatiya Institute of Technology and Science, Opp Yerragattu Hillock Bheemaram Village, Hasanparthy Mandal, Koukonda, 506015 Warangal, India

²Department of Electrical and Electronics Engineering,

B V Raju Institute of Technology Hyderabad College Of Engineering For Women, Plot No. 8-5/4, Rajiv Gandhi Nagar Colony, Nizampet Rd, Bachupally, 500090 Hyderabad, India

sravyakedari15@gmail.com, vrg.eee@kitsw.ac.in, amritha.k@bvrithyderabad.edu.in

DOI: 10.15598/aeee.v19i4.4227

Article history: Received May 16, 2021; Revised Nov 02, 2021; Accepted Nov 07, 2021; Published Dec 31, 2021. This is an open access article under the BY-CC license.

Abstract. *This paper deals with a system that consists of a combination of wind and solar sources. The wind energy unit is the primary energy source that feeds the load and is controlled by the $I \cos \Phi$ algorithm. The algorithm's efficiency is tested under normal operation and when one of the phases in the load is disconnected. This algorithm efficiently maintains the voltage and frequency during these conditions. The solar unit is directly connected with the battery energy storage system and is used to charge the battery. It implements MPPT using Perturb and Observe (P&O) method. The hybrid system is simulated in MATLAB/SIMULINK. It is found to perform and maintain the frequency and the potential at the load side and the point of common coupling under normal operation and varying load conditions. $I \cos \Phi$ algorithm, which controls the switching signals, requires simple calculations for generating reference source currents. This algorithm does not need conversion from one frame to another, making the system respond for quick dynamics and improved power quality. The perturb and observe method is proven to ensure the maximum power extraction from the solar panel. Thus, the combination of these two techniques makes the system act efficiently and handle load disturbances.*

Keywords

Wind energy unit, solar energy conversion system, control algorithm, Maximum Power Point Tracking (MPPT), Perturb and Observe algorithm.

1. Introduction

The need for renewable energy sources for energy production is becoming more and more significant in recent years. Solar and wind are two resources that are available in abundance universally. The green and clean energy output have made these two fields popular. A combination of wind and solar can be a part of the microgrid, which is used in areas where the grid connection is not a viable option.

A lot of literature is available regarding the control of wind units and solar units separately and as a hybrid unit. The implementation of the $I \cos \Phi$ algorithm in different applications are also mentioned in many articles. [1] gives information on variable generators in his Electrical generator handbook. [2] give various methods for Power system quality Assessment. IEEE recommended practices for power quality standards are mentioned in [3] and [4]. [5] designed and executed the $I \cos \Phi$ algorithm for shunt active filter. [6] proposed a newer version of the $I \cos \Phi$ algorithm called Levenberg-Marquardt using backpropagation. In [7] and [8], the authors explain the (P&O) based MPPT technique under different weather conditions and different applications.

[10] designed a DSTATCOM using Naive backpropagation based $I \cos \Phi$. [11] present a review on different renewable energy powered water pumping systems. The advantage of each method and the control strategies used in the power electronic interface are discussed here. [12] simulated a tandem solar cell with more than 41 % efficiency. [13] proposed ma-

chine learning-based PV generation forecasting. The forecasting performance is analyzed by using different Machine Learning (ML) techniques. The maximum power extraction based on the artificial bee colony optimization technique is proposed, which is proven superior to the P&O method [14]. [15] suggested a hybrid DC/AC microgrid with various maximum power extraction strategies. [16] presents a review on DC microgrid's planning, operation, and control. [17] developed and investigated various Deep Neural Network models to predict solar irradiance one day ahead. [18] suggested detecting the PV cell failures based on the voltage and current signals produced due to the electrical interaction of different parameters. [19] propose a salp swarm based MPPT for the solar unit, which works efficiently under dynamic weather conditions. [20] uses HOMER software to perform sensitivity analysis and evaluate technical and financial feasibilities. [21] present the application of the $I \cos \Phi$ algorithm in small hydropower generating station. It proves the algorithm's effectiveness in controlling the terminal voltage and frequency and in mitigating the harmonics. [22] present an improved ATILS control strategy based on Adaptive theory for Power Quality improvement using Dynamic Voltage Restorer (DVR), which is very efficient for mitigating the harmonics. [23] give an insight into a neural network-based control for a grid-connected solar photovoltaic (PV) system.

The proposed system is a combination of a wind energy conversion unit and a solar energy unit. The solar unit is connected directly to the battery. To ensure that the solar panel gives out the maximum power, the MPPT technique Perturb and Observe method is used. The wind power unit is controlled by the $I \cos \Phi$ algorithm. The switching of Insulated Gate Bipolar Transistors (IGBTs) in the voltage source converter is controlled by the triggering signals produced according to this algorithm. $I \cos \Phi$ algorithm requires simple calculations for the generation of reference source currents. This algorithm does not require any conversion from one frame to another, making the system respond for quick dynamics and improved power quality. The star-delta transformer suppresses the neutral current and reduces the DC link voltage and voltage rating of the Voltage Source Converter (VSC).

2. Wind and Solar Power Systems

2.1. Wind Energy Conversion System

A wind generator converts the mechanical energy fed to it by the wind turbine to electrical energy. The wind output varies proportionately to the cube of the wind velocity. It is found that only 59 % of the wind power input is getting converted to the output.

The characteristics of the wind output power against the turbine speed for different values of windspeeds is as shown in Fig. 1 that as the turbine speed increases, turbine output power increases, becoming maximum at a particular speed. The output power decreases if the turbine speed increases further.

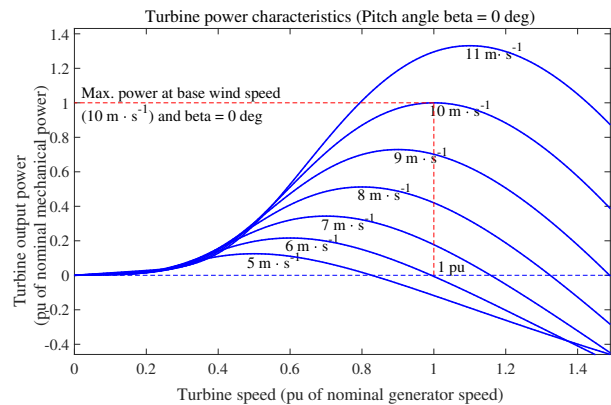


Fig. 1: Turbine output power characteristics.

The output power equation for the wind generator is derived from the fact that the kinetic energy of a body depends upon the mass and velocity. Power is the rate of change of energy. The output power equation can be given by:

$$P = \frac{1}{2} \rho A V^3, \quad (1)$$

where P is the power extracted from the wind expressed in watts, ρ is the air density in $\text{kg}\cdot\text{m}^{-3}$, A is the swept area of the blade in m^2 and V is the wind velocity in $\text{m}\cdot\text{s}^{-1}$. Eq. (1) calculates the maximum energy that can be transformed from the wind, but the Betz condition sets a limit to the extracted energy because wind movement is not stopped after hitting the wind blades. Thus, even though the equation gives a significant value for the power converted, the actual power converted to electrical energy is less than 50 % of the calculated value. And so, the generators are rated at a much lesser value than the calculated one.

2.2. Solar Photo Voltaic System

In a solar energy conversion system, a photovoltaic cell converts the energy in the sun rays to electricity or heat energy. The efficiency of the solar cell is only around 17 %, and it depends on the temperature of the solar cell, the quantity of sunlight falling on it and the load characteristics. The disadvantage with solar energy is, it changes with the weather conditions which makes a fully dependent solar powered system to be less reliable. But the development of appropriate energy storage systems has allowed this energy conversion to be very economical.

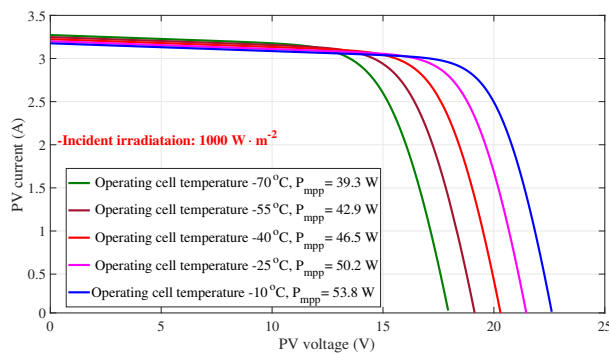


Fig. 2: PV cell voltage to current relationship for different temperatures.

Figure 2 shows the V-I characteristics of a solar cell with temperature. In a solar cell, the temperature has a profound effect on the voltage generated. If the temperature is increased above this limit, that causes a reduction in voltage.

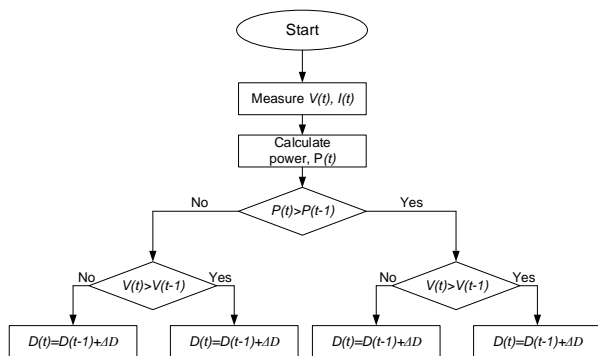


Fig. 3: P&O algorithm for MPPT.

Figure 3 shows the flowchart for the MPPT algorithm. The flowchart shows that the duty cycle is set according to the value of the power extracted from the system. If the extracted power is greater than the power extracted in the previous time instant, then the voltage is reversed. Or, if the power is lesser than the power drawn at the previous instant, then the voltage is kept as it is. So, the power drawn can be adjusted

to the maximum value by adjusting the duty cycle in the DC-to-DC converter.

3. System Configuration

The circuit under consideration is a combination of wind and solar energy conversion units. Figure 4 shows the schematic diagram of the wind energy generating unit. The wind Generator is directly connected to the load. The solar system is used as a backup for charging the battery.

The wind generator unit uses a 7.5 kW, 415 V, 50 Hz asynchronous generator to generate electricity. A delta connected capacitor circuit of 8 kVAR capacity generates the necessary reactive power for the generator. A star-delta transformer couples the controller with the load circuit. The neutral of the star connected side of the transformer is connected with load neutral so that the neutral current which flows in case of unbalance will circulate in this connection, and it will not affect the source neutral.

The solar energy system uses a photovoltaic panel having 34 cells connected in series producing a total open-circuit voltage of 64.2 V. Two modules are connected in series, and six modules in parallel. As mentioned earlier, the efficiency of the PV modules is significantly less. A step towards improving the efficiency is done by operating the photovoltaic cells using the maximum power point technique. And as a result, the panel generates maximum power. Perturb and Observe is the MPPT technique used here.

A battery is used, which maintains the dc-link voltage at a constant level. Wind power and solar power are used to charge the battery. The battery helps the system to maintain stability under abnormal conditions. The battery absorbs the unused power and gets recharged whenever the load is less than the rated load. In case if the load is increased, the battery provides the extra power and thus helps the system handle the uncertainty in the load.

4. Control Algorithm

4.1. Calculation of Reference Currents in Wind System

The in-phase and quadrature components of the reference currents are calculated based on the principles of $I \cos \Phi$ algorithm. Figure 5 explains this algorithm in detail. The terminal voltage is given as:

$$V_{tv} = \sqrt{\frac{2}{3} (V_{va}^2 + V_{vb}^2 + V_{vc}^2)} \tag{2}$$

The unit templates in phase are found out as:

$$U_{ta} = \frac{V_{va}}{V_{tv}}, U_{tb} = \frac{V_{vb}}{V_{tv}}, U_{tc} = \frac{V_{vc}}{V_{tv}}. \quad (3)$$

The real component values of load current are given by:

$$\begin{aligned} I_{Lpa} &= I_{Las} \cos \Phi_{as}, \\ I_{Lpb} &= I_{Lbs} \cos \Phi_{bs}, \\ I_{Lpc} &= I_{Lcs} \cos \Phi_{cs}, \end{aligned} \quad (4)$$

where Φ_{as} , Φ_{bs} and Φ_{cs} are the angles between the load voltages and load currents.

The frequency of the load voltage is measured and compared with the standard value of frequency and the difference is given out as the error. This difference at any instant is given as:

$$f_{de}(nt) = f_{ref} - f(nt). \quad (5)$$

The PI controller output is given by:

$$\begin{aligned} I_{fp}(nt) &= I_{fp}(nt-1) + \\ &+ K_{fp}\{f_{de}(nt) - f_{de}(nt-1)\} + K_{fi}f_{de}(nt). \end{aligned} \quad (6)$$

The magnitude of the real component of reference current is given by:

$$I_{pr} = I_{fp} + I_{Lpr}, \quad (7)$$

where,

$$I_{Lpr} = \frac{(I_{Lpa} + I_{Lpb} + I_{Lpc})}{3}. \quad (8)$$

Thus, the active components of reference source current are given by:

$$\begin{aligned} I_{sap}^* &= I_{pr}u_{ta}, \\ I_{sbp}^* &= I_{pr}u_{tb}, \\ I_{scp}^* &= I_{pr}u_{tc}. \end{aligned} \quad (9)$$

The quadrature components of source current are found by finding the product of the quadrature component of the unit template with the magnitude of the reactive components of reference currents. The quadrature components of unit templates are found out:

$$\begin{aligned} w_{ta} &= \frac{-u_{tb}}{\sqrt{3}} + \frac{u_{tc}}{\sqrt{3}}, \\ w_{tb} &= \frac{\sqrt{3}}{2}u_{ta} + \frac{u_{tb}}{2\sqrt{3}} - \frac{u_{tc}}{2\sqrt{3}}, \\ w_{tc} &= \frac{-\sqrt{3}}{2}u_{ta} + \frac{u_{tb}}{2\sqrt{3}} - \frac{u_{tc}}{2\sqrt{3}}. \end{aligned} \quad (10)$$

The terminal voltage is measured and compared with the standard value and difference is termed as the error voltage.

$$V_{te}(n) = V_{tref}(n) - V_t(n). \quad (11)$$

The PI controller output is given by:

$$I_{vq}(nt) = I_{vq}(nt-1) + K_{vp}\{V_e(nt) - V_e(nt-1)\} + K_{vi}V_e(nt). \quad (12)$$

The quadrature component of source current is given by:

$$I_q = I_{vq} - I_{Lq}, \quad (13)$$

where,

$$I_{Lq} = \frac{I_{Lqa} + I_{Lqb} + I_{Lqc}}{3}. \quad (14)$$

Thus, the reactive components of reference source current are given by:

$$\begin{aligned} I_{sqa}^* &= I_{Lq}u_{aq}, \\ I_{sqb}^* &= I_{Lq}u_{bq}, \\ I_{sqc}^* &= I_{Lq}u_{cq}. \end{aligned} \quad (15)$$

The reference current for each phase is given by the equation:

$$\begin{aligned} I_{as}^* &= I_{sap}^* + I_{sqa}^*, \\ I_{bs}^* &= I_{sbp}^* + I_{sqb}^*, \\ I_{cs}^* &= I_{scp}^* + I_{sqc}^*. \end{aligned} \quad (16)$$

These reference currents are compared with the measured values of source currents, and the gating signal for the voltage source converter is produced based on the error signal.

4.2. Equations Pertaining to Solar Energy Conversion

A solar cell can be considered as a current source, with a diode connected in parallel. The maximum power that can be delivered by a solar cell is given by the equation:

$$P = V_{OC} \cdot I_{OC} \cdot ff, \quad (17)$$

where ff is the fill factor which characterizes the non-linear electrical behavior of the solar cell. The maximum power extracted from the cell depends upon its characteristic resistance, which in turn depends upon the temperature, illumination and the age of the cell. This resistance is adjusted in a way that the maximum power is produced.

The equivalent circuit of a solar cell is given in Fig. 6. From the Fig. 6, the output current is given by:

$$I = I_{sc} - I_d - I_{sh}, \quad (18)$$

$$I = I_{sc} - \frac{V + IR_s}{R_{sh}} - I_0 \left(e^{\left(\frac{V + IR_s}{nV_t} \right)} - 1 \right), \quad (19)$$

where R_s is the internal series resistance, R_{sh} is the parallel internal resistance, V_t is the thermal voltage, I_{sc} is the short circuit current, I_0 is the reverse saturation current, n is the ideality factor of the diode.

If the shunt resistance is neglected:

$$I = I_{sc} - I_0 \left(e^{\left(\frac{V + IR_s}{nV_t} \right)} - 1 \right). \quad (20)$$

PV cell output voltage can be given by:

$$V = -IR_s + \frac{AKT}{q} \ln \frac{I_{sc} + I_0 - I}{I_0}. \quad (21)$$

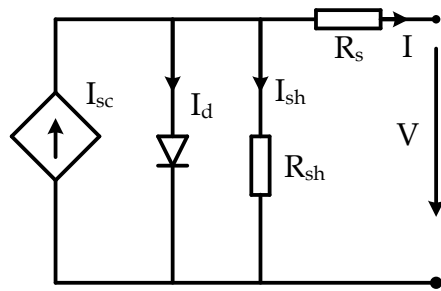


Fig. 6: Equivalent circuit of a solar cell.

In Perturb and Observe method of MPPT technique, a power variation is created in the module by introducing a small perturbation. The output power of the solar panel is measured and compared with the formerly measured power. If the output power is found to have an increased value, the perturbation is continued. If it has a lower value compared to the previous one, perturbation is reversed.

5. Results and Discussions

As mentioned earlier, the system uses a wind power unit as the primary power source for the load. The load is connected to the source at 0.35 seconds. The controller is connected at 0.5 seconds. It is found that the controller brings the system into stability within a second. The load is disconnected at 6.65 seconds and gets reconnected at 6.75 seconds.

Figure 7 displays the generated voltage, generated current, load current, the current from the compensator, voltage, battery voltage, battery current, source neutral current at the point of common coupling, load neutral current and frequency during the load disconnection for a linear load. It is clear from the waveform that when the load is removed at 6.6 seconds, the source current is unaffected. It still maintains the sinusoidal waveform as the controller compensates for the fluctuations in the load current.

The battery voltage also remains constant. The positive values of battery current indicate that the battery charges during load reduction. This battery operation helps the system maintain its stability. The controller controls the small changes in the frequency during the disconnection and reconnection.

Figure 8 shows the waveforms for a nonlinear load. The generated voltage generated current, load current, the current from the compensator, PCC voltage, battery voltage, battery current, source neutral current, load neutral current and frequency when the load is removed from the circuit are plotted. It is found that the controller is working efficiently even for the nonlinear load.

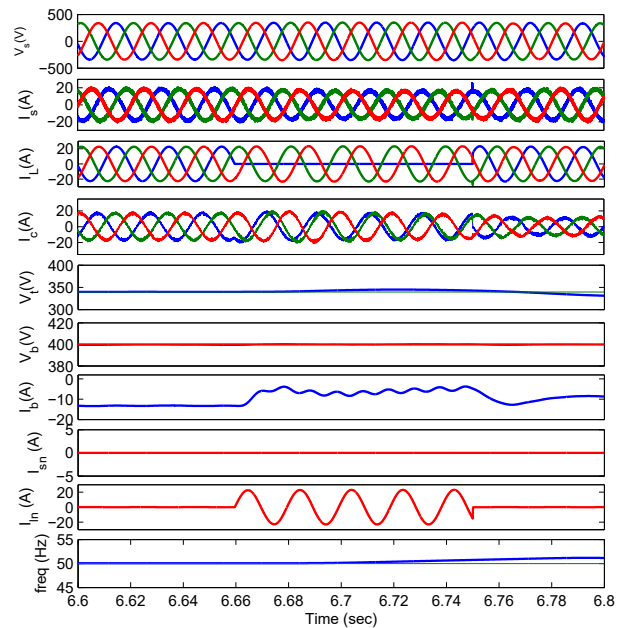


Fig. 7: Waveforms during load disconnection for a linear load.

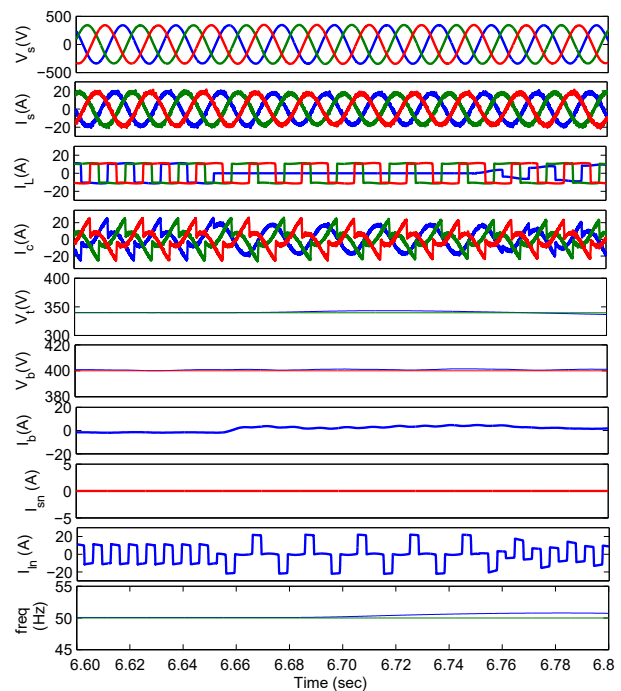


Fig. 8: Waveforms during load disconnection for a nonlinear load.

Figure 9 shows the changes in the current, voltage and power produced in the solar panel with the changes in irradiance. The voltage and the current are seen fluctuating with a change in irradiance. But due to the action of the MPPT algorithm, these variations are kept within limits so that the maximum power is extracted from the circuit.

Figure 10 shows the Total Harmonic Distortion (THD) in the source voltage and source current during

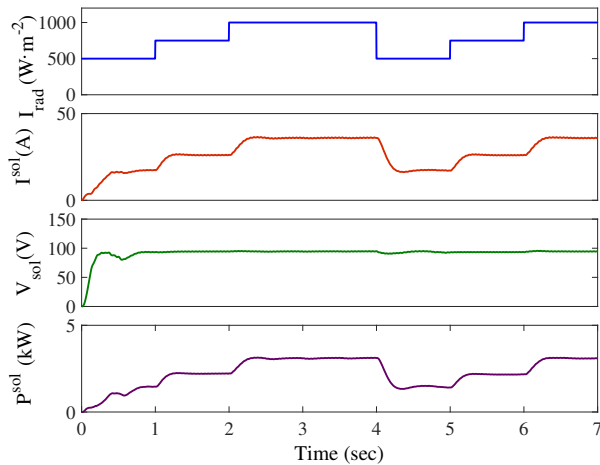


Fig. 9: Solar irradiance, voltage and current.

the period when the load is disconnected and reconnected. The THD in source voltage is 0.41 % and in the current waveform it is 4.72 % which are well within the limit permitted by IEEE 519 standards.

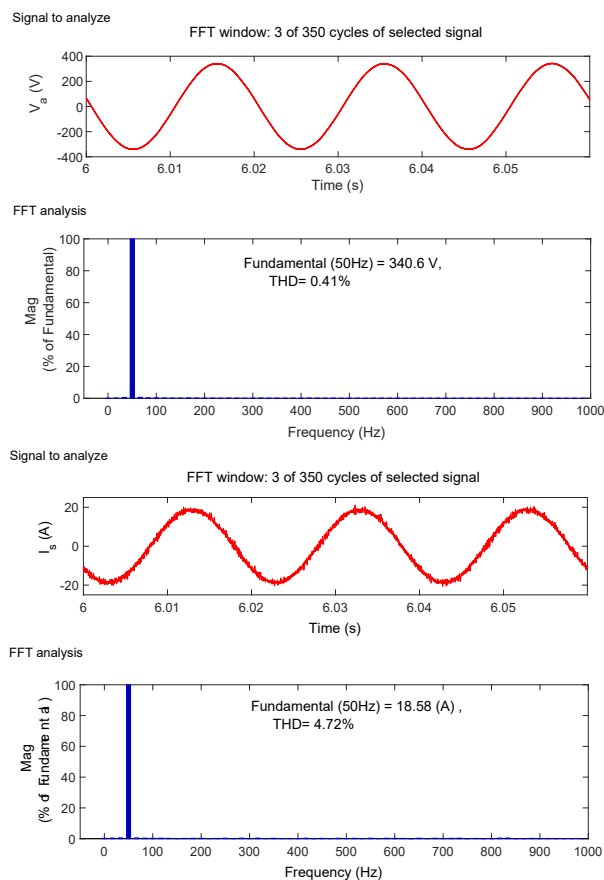


Fig. 10: THD in source voltage and current.

6. Conclusion

The performance of a wind energy conversion system that supplies power to a nonlinear load is analyzed. The action of a solar energy source to charge the battery is studied. The wind unit is controlled by a controller that uses the $I \cos \Phi$ algorithm to regulate the system parameters in case of variation in load. This algorithm is found to work effectively and maintains the system parameters within acceptable limits. The addition of a solar energy source is found to act as an effective backup for the system. The Perturb and Observe method acts as an excellent technique for maximum power extraction.

Author Contributions

S.K. has contributed in simulation of the circuit. A.K. has contributed in documentation. R.V. has supervised the project and guided in all aspects.

References

- [1] BOLDEA, I. *Variable Speed Generators (The Electric Generators Handbook)*. 1st ed. New York: CRC Press, 2005. ISBN 978-0-849-35715-2.
- [2] ARILLAGA, J., N. R. WATTSON and S. CHEN *Power System Quality Assessment*. 1st ed. New York: John Wiley & Sons, 2000. ISBN 978-0-471-98865-6.
- [3] IEEE Std 519-1992. *IEEE Recommended Practices and Requirements for Harmonic Control in Electrical Power Systems*. New York: IEEE, 1993.
- [4] IEEE Std 141-1993. *IEEE Recommended Practice for Electric Power Distribution for Industrial Plants*. New York: IEEE, 1994.
- [5] BHUVANESWARI, G. and M. G. NAIR. Design, Simulation, and Analog Circuit Implementation of a Three-Phase Shunt Active Filter Using the $I \cos \Phi$ Algorithm. *IEEE Transactions on Power Delivery*. 2008, vol. 23, iss. 2, pp. 1222–1235. ISSN 1937-4208. DOI: 10.1109/TPWRD.2007.908789.
- [6] MANGARAJ, M., A. K. PANDA, T. PENTHIA and A. R. DASH. Adaptive LMBP training-based $I \cos \Phi$ control technique for DSTATCOM. *IET Generation, Transmission & Distribution*. 2020, vol. 14, iss. 3, pp. 516–524. ISSN 1751-8695. DOI: 10.1049/iet-gtd.2018.6295.

- [7] AZAD, M. L., S. DAS, P. K. SADHU, B. SATPATI, A. GUPTA and P. ARVIND. P&O algorithm based MPPT technique for solar PV system under different weather conditions. In: *International Conference on Circuit, Power and Computing Technologies (ICCPCT)*. Florence: IEEE, 2017, pp. 1–5. ISBN 978-1-5090-4967-7. DOI: 10.1109/ICCPCT.2017.8074225.
- [8] KAMRAN, M., M. MUDASSAR, M. R. FAZAL, M. U. ASGHAR, M. BILAL and R. ASGHAR. Implementation of improved Perturb & Observe MPPT technique with confined search space for standalone photovoltaic system. *Journal of King Saudy University – Engineering Sciences*. 2020, vol. 32, iss. 7, pp. 432–441. ISSN 1018-3639. DOI: 10.1016/j.jksues.2018.04.006.
- [9] SALMAN, S., X. AI and Z. WU. Design of a P-&O algorithm based MPPT charge controller for a stand-alone 200W PV system. *Protection and Control of Modern Power Systems*. 2018, vol. 3, iss. 1, pp. 1–8. ISSN 2367-2617. DOI: 10.1186/s41601-018-0099-8.
- [10] MANGARAJ, M. and A. K. PANDA. NBP-based $i \cos \Phi$ control strategy for DSTATCOM. *IET Power Electronics*. 2017, vol. 10, iss. 12, pp. 1617–1625. ISSN 1755-4543. DOI: 10.1049/iet-pel.2017.0129.
- [11] ANGADI, S., U. R. YARAGATTI, Y. SURESH and A. B. RAJU. Comprehensive review on solar, wind and hybrid wind-PV water pumping systems-an electrical engineering perspective. *CPSS Transactions on Power Electronics and Applications*. 2021, vol. 6, iss. 1, pp. 1–19. ISSN 2475-742X. DOI: 10.24295/CPSSSTPEA.2021.00001.
- [12] MOUSA, M., F. Z. AMER, R. I. MUBARAK and A. SAEED. Simulation of Optimized High-Current Tandem Solar-Cells with Efficiency Beyond 41%. *IEEE Access*. 2021, vol. 9, iss. 1, pp. 49724–49737. ISSN 2169-3536. DOI: 10.1109/ACCESS.2021.3069281.
- [13] MAHMUD. K., S. AZAM, A. KARIM, S. M. ZOBAED, B. SHANMUGAM and D. MATHUR. Machine Learning Based PV Power Generation Forecasting in Alice Springs. *IEEE Access*. 2021, vol. 9, iss. 1, pp. 46117–46128. ISSN 2169-3536. DOI: 10.1109/ACCESS.2021.3066494.
- [14] CASTANO, C. G., C. RESTREPO, S. KOURO and J. RODRIGUEZ. MPPT Algorithm Based on Artificial Bee Colony for PV System. *IEEE Access*. 2021, vol. 9, iss. 1, pp. 43121–43133. ISSN 2169-3536. DOI: 10.1109/ACCESS.2021.3066281.
- [15] SOUNDARYA, G., R. SITHARTHAN, C. K. SUNDARABALAN, C. BALASUNDAR, D. KARTHIKAIKANNAN and J. SHARMA. Design and Modeling of Hybrid DC/AC Microgrid With Manifold Renewable Energy Sources. *IEEE Canadian Journal of Electrical and Computer Engineering*. 2021, vol. 44, iss. 2, pp. 130–135. ISSN 2694-1783. DOI: 10.1109/ICJECE.2020.2989222.
- [16] FAHAD, S. DC Microgrid Planning, Operation, and Control: A Comprehensive Review. *IEEE Access*. 2021, vol. 9, iss. 1, pp. 36154–36172. ISSN 2169-3536. DOI: 10.1109/ACCESS.2021.3062840.
- [17] BOUBAKER, S., M. BENGHANEM, A. MELLIT, A. LEFZA, O. KAHOULI and L. KOLSI. Deep Neural Networks for Predicting Solar Radiation at Hail Region, Saudi Arabia. *IEEE Access*. 2021, vol. 9, iss. 1, pp. 36719–36729. ISSN 2169-3536. DOI: 10.1109/ACCESS.2021.3062205.
- [18] REYES, M.-A. Z., J.-B. R. OCAMPO, P.-Y. S. CAMACHO, J. R. RESENDIZ, O. L. DANGUILLECOURT and J.-E. C. DIAZ. Photovoltaic Failure Detection Based on String-Inverter Voltage and Current Signals. *IEEE Access*. 2021, vol. 9, iss. 1, pp. 39939–39954. ISSN 2169-3536. DOI: 10.1109/ACCESS.2021.3061354.
- [19] SAWLE, Y., S. JAIN, S. BABU, A. R. NAIR and B. KHAN. Prefeasibility Economic and Sensitivity Assessment of Hybrid Renewable Energy System. *IEEE Access*. 2021, vol. 9, iss. 1, pp. 28260–28271. ISSN 2169-3536. DOI: 10.1109/ACCESS.2021.3058517.
- [20] JAMALUDIN, M. N. I., M. F. N. TAJUDIN, J. AHMED, A. AZMI S. A. AZMI, N. H. GHAZALI, T. S. BABU and H. H. ALHELOU. An Effective Salp Swarm Based MPPT for Photovoltaic Systems Under Dynamic and Partial Shading Conditions. *IEEE Access*. 2021, vol. 9, iss. 1, pp. 34570–34589. ISSN 2169-3536. DOI: 10.1109/ACCESS.2021.3060431.
- [21] GOPAL, V. R. and B. SINGH. Decoupled Electronic Load Controller for Off grid Induction Generators in Small Hydro Power Generation. *International Journal of Emerging Electric Power Systems*. 2011, vol. 12, iss. 1, pp. 1–12. ISSN 1553-779X. DOI: 10.2202/1553-779X.2638.
- [22] BANGARRAJU, J., V. RAJAGOPAL, S. R. ARYA and B. SUBHASH. Enhancement of PQ Using Adaptive Theory based Improved Linear Tracer Sinusoidal Control Strategy for DVR. *Journal of Green Engineering*.

2017, vol. 7, iss. 1, pp. 189–212. ISSN 1904-4720. DOI: 10.13052/jge1904-4720.7129.

- [23] PRAGATHI, B., R. VERAMALLA, F. NOORBASHA and B. JAMPANA. Power quality improvement for grid interconnected solar PV system using neural network control algorithm. *International Journal of Power and Energy Conversion*. 2018, vol. 9, iss. 2, pp. 187–204. ISSN 1757-1162. DOI: 10.1504/IJPEC.2018.090684.

About Authors

Sravya KEDARI received her bachelor's degree from SR University, Warangal in the stream of Electrical and electronics engineering. Presently, she is pursuing her masters in power electronics and drives at Kakatiya Institute of Technology and Science, Warangal. Her areas of interest include renewable energy sources for power generation and Wind and solar integrated energy systems.

Rajagopal VERAMALLA received the AMIE (Electrical) degree from The Institution of Engineers (India), M.Tech. Degree from the Uttar Pradesh Technical University, India and Ph.D. degree in

Indian Institute of Technology (IIT) Delhi. Presently, working as a Professor of Electrical & Electronics Engineering, Kakatiya Institute of Technology and Science, Warangal, Telangana, India. His areas of interest include power electronics and drives, renewable energy generation and applications, Flexible AC Transmission Systems (FACTS), and power quality. He has one patent, 20 International & National Journals and 34 IEEE and National conferences held in India and abroad. He is a life member of the Indian Society for Technical Education (ISTE) and a Fellow of the Institution of Engineers (India).

Amritha KODAKKAL (corresponding author) received her B.E. degree in Electrical & Electronics Engineering from Karnataka Regional Engineering College, Surathkal (presently National Institute of Technology (NIT), Surathkal), and M.Tech. from Jawaharlal Nehru Technological University Hyderabad, India. She is working as an Associate Professor in B V Raju Institute of Technology (BVRIT) Hyderabad College of Engineering for Women, Hyderabad. She is currently pursuing her Ph.D. at Koneru Lakshmaiah deemed to be University, in the field of Power Quality improvement in Wind Energy Conversion Systems. Her research interest include power electronic converters, renewable energy sources and power quality.